Original Research

The Synergetic Effects in a Fenton-like System Catalyzed by Nano Zero-valent Iron (nZVI)

Hairui Yao, Sihai Hu, Yaoguo Wu*, Lin Fan

Department of Chemistry, Northwestern Polytechnical University, Xi'an, Shaanxi, China

Abstract

In this study, the synergetic effects in a Fenton-like system catalyzed by nano zero-valent iron (nZVI Fenton-like system) were studied using nitrobenzene (NB) as a model contaminant. The results showed that homogeneous and heterogeneous Fenton processes existed simultaneously in the nZVI Fenton-like system, and a synergetic removal effect between these processes played a considerable role in NB removal. Through quantitative analysis, 36.5% of NB degradation was attributed to the synergetic degradation effect, which was caused by a synergetic catalytic effect between nZVI and dissolved iron ions (Fe^{3+} and Fe^{2+}). In the bulk solution, the Fe^{3+}/Fe^{2+} redox rate was accelerated by nZVI, resulting in the efficiency improvement of homogeneous catalysis; in the surface of nZVI, these dissolved iron ions promoted the electrons transfer from nZVI core to shell, enhancing the efficiency of heterogeneous catalysis. The synergetic catalytic effect also improved the utilization-rate of H_2O_2 by reducing the decomposition caused by Fe^{3+}/Fe^{2+} redox compared to that in the homogeneous Fenton system. Based on these results, a possible mechanism of synergetic effects in the nZVI Fenton-like system was proposed. These results could provide insight into an nZVI Fenton-like system.

Introduction

Heterogeneous Fenton has emerged as a promising technique for advanced oxidation processes and has attracted great attention in environmental modification due to its intrinsic advantages over classical homogeneous Fenton, such as widely effective pH range, less iron sludge, and lower amount of H_2O_2 consumption [1-5]. Many solid catalysts containing iron, like Fe_2O_3 [6, 7], FeS_2 [8, 9], FeOOH [10-12], and Fe_3O_4 [13, 14], have been seen to be effective in heterogeneous Fenton treatment of various organics in water. In particular, nano zero-valent iron (nZVI, Fe^0) has been chosen as an effective catalyst in environmental remediation because it has a smaller size and thus large specific surface areas, facilitating greater reaction rates compared to bulk or micro-scale iron materials [15-17]. Therefore, extensive efforts have been directed to assess the potential application of nZVI for decomposing organic pollutants as catalysts in heterogeneous Fenton-like systems [15, 18-20]. However, little insight into the catalysis mechanism of nZVI has been provided in a heterogeneous Fenton-like system. To date, views are

*e-mail: wuygal@163.com

mixed regarding the actual mechanism of heterogeneous Fenton-like system catalyzed by nZVI.

It is known that nZVI has a strong tendency to become oxidized [21, 22]. Devi et al. [23] described how nZVI in a Fenton-like system released ferrous ion (Fe^{2+}) to the bulk solution in the presence of hydrogen peroxide (H_2O_2) and H^+(Eq.(1)), and then the Fe^{2+} catalyzed H_2O_2 to produce hydroxyl radical (HO·) (Eq. 2), resulting in a homogeneous Fenton process [24].

$$Fe^0 + H_2O_2 + 2H^+ \rightarrow Fe^{2+} + 2H_2O \quad (1)$$

$$Fe^{2+} + H_2O_2 \rightarrow Fe^{3+} + OH^- + HO· \quad (2)$$
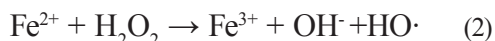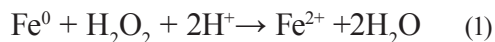
This homogeneous Fenton mechanism seems reasonable, focusing on the reduction of nZVI and catalysis of the Fe^{2+}. However, it failed to explain the lower concentration of Fe^{2+} and the wider effective pH range in a Fenton-like system catalyzed by nZVI compare to a traditional Fenton system.

In contrast to the above homogeneous Fenton mechanism, several authors have reported that a real heterogeneous Fenton process occurred [25]. The HO· could be generated by decomposition of H_2O_2 on the surface of catalysts through a chain reaction mechanism. Electrons were transferred from iron core to surface, and result in an H_2O_2 activation process [26, 27]. This mechanism offered an explanation for the lower concentration of Fe^{2+} and the wider effective pH range. However, this mechanism ignored the problem of the corrosion of catalysts and the diffusion rates of H_2O_2 to the catalyst surface.

These mechanisms under discussion provide promising insight into the simultaneous existence of homogeneous and heterogeneous Fenton processes in a Fenton-like system catalyzed by nZVI. Both processes work on the removal of target pollutants. With further study, a synergetic effect was found on the coexistence of nZVI and dissolved iron ions. Shi et al. [28] reported that nZVI could accelerate the Fe^{3+}/Fe^{2+} cycles in the bulk solution, which means the efficiency of homogeneous Fenton was enhanced by nZVI. On the other hand, Liu et al. [29] suggested that the dissolved Fe^{2+} could promote the production of reactive oxygen species via surface-bound ferrous ions ($Fe(II)_{bound}$). Obviously, there were similar conditions when nZVI was used as Fenton catalyst, so it was more likely that synergetic effects may exist in a heterogeneous Fenton-like system catalyzed by nZVI. However, few studies, to our knowledge, have been carried out on synergetic effects in a heterogeneous Fenton-like system catalyzed by nZVI, which would further elucidate the catalysis mechanism of nZVI.

Therefore, in this study, the synergetic effects were studied using synthesized nZVI as a Fenton catalyst. Nitrobenzene (NB), which is widely used as a raw material and refractory to biological treatments or conventional chemical oxidation, was selected as the model target contaminant. The degradation of NB with homogeneous Fenton processes as well as heterogeneous Fenton process was investigated in a Fenton-like system catalyzed by nZVI. A series of experiments were also designed to reveal the synergetic effect between the processes, as well as the synergetic effect between nZVI and dissolved iron ions in some details to propose a proper catalysis mechanism.

Experimental

Materials and Chemicals

Nitrobenzene (NB, purity higher than 99.0%), ferrous sulphate heptahydrate ($FeSO_4·7H_2O$, purity higher than 99%), NaOH (purity higher than 96%), and HCl (36%~38%) were purchased from Sinopharm Chemical Reagent Shanghai Co., Ltd. (Shanghai, China). Sodium borohydride ($NaBH_4$, purity higher than 98%), hydrogen peroxide (H_2O_2, non-stabilized, 30%), ethylene diamine tetraacetic acid (EDTA, purity higher than 99%), and methanol (purity higher than 99%) were acquired from the First Chemical Reagent Manufactory (Tianjin China). Aqueous solutions for the experiment were prepared with deionizer water. High-purity argon was used to make anoxic conditions. An NB stock solution was prepared by dissolving 0.4 g NB in 1.0 L of deionized water, and a working solution with designed concentrations was prepared by diluting the stock solution.

Preparing nZVI

The nZVI used in this study was synthesized by aqueous-phase reduction of $FeSO_4$ solution using $NaBH_4$ as a reducing agent [30]. According to this method, $FeSO_4·7H_2O$ was dissolved and stirred with an electric rod for 15 min in an argon atmosphere, and then the $NaBH_4$ aqueous solution was added dropwise. After adding all of the $NaBH_4$ solution, the mixture was stirred under the argon atmosphere continuously for another 20 min. The reduction reaction process could be represented as the following Eq.(3):

$$Fe^{2+} + 2BH_4^- + 6H_2O \rightarrow Fe^0 \downarrow + 2B(OH)_3 + 7H_2 \uparrow \quad (3)$$
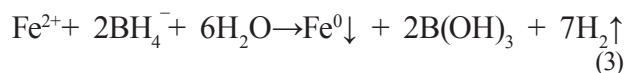
After sufficient reduction, the solids were collected through a vacuum filtration flask with 0.45 μm micro porous membrane filter, and then were rinsed three times with degassed deionized water. Finally, the solids were dried at 60°C under vacuum for instant usage.

Characterizations and Methods

Morphology and size of nZVI were observed with a scanning electron microscope (SEM, VEGA 3 LMH, TESCAN, Czekh). The energy dispersive

was determined through x-ray energy dispersive spectrometry (EDS, Oxford INCA X-ACT equipment in SEM). The element characteristics of nZVI were obtained using x-ray photoelectron spectroscopy (XPS, Axis Ultra DLD, Kratos, UK) with Al Kα radiation. Core-level spectra for O1s and Fe2p were taken at high resolution, and analyzed for chemical state information. Crystal structure of the solids was examined by an x-ray diffractmeter (XRD, Model D8, Bruker, Germany) with Cu Kα1 radiation (k = 0.154 nm). The XRD patterns were recorded in the range of 2θ = 10-80º. The instrument was operated at 40 kV and 30 mA, and the spectra were recorded at a scanning speed of 1º/min(2θ) and a step of 0.01 nm.

Batch Experiments

Batch degradation experiments were designed to look into the apparent removal of NB in a Fenton-like system catalyzed by nZVI. Experiments were carried out in glass vessels at ambient temperature under dark and anoxic conditions. The stock solution of NB was diluted into 40 mgL^{-1} as model wastewater samples. The initial solution pH values were adjusted with 1.0 molL^{-1} HCl and 1.0 molL^{-1} NaOH. All solutions were thoroughly stirred to make them well-distributed through a rotary shaker (TZ-2EH, Beijing Wode Company) at 150 rpm during the entire experimental period.

The reaction was started by adding H_2O_2 to the reaction mixture. Samplings were taken regularly and mixed immediately with ethanol to quench the reaction. The samples additionally were filtered through 0.45 μm membrane filters to separate solids from the solution for analysis.

All these experiments were carried out in triplicate and the mean values and standard deviations are presented, and analyses showed that relative errors were lower than ±5%.

SampleAnalysis

The concentrations of NB were determined using high-performance liquid chromatography (HPLC) equipped with a waters symmetry C-18 column (150 mm × 4.6 mm i.d., 5 μm). The mobile phase was the mixture of methanol and 5 mM H_3PO_4 in a ratio of 3:2 (v/v). The flow rate was set at 1 mLmin^{-1}, and the detection wavelength was set to 267.5 nm [31, 32].

The concentration of dissolved ferrous ions was measured by the 1,10-phenanthrolin method, and the total dissolved iron ions was quantified after adding hydroxylamine hydrochloride to the filtered solution. Samples were analyzed at max wavelength of 510 nm by a UV-visible spectrophotometer (UV-2550, Shimadzu, Japan).

H_2O_2 was analyzed with the N,N-diethyl-p-phenylene-diamine(DPD) method modified to minimize the interference by Fe^{2+} and Fe^{3+} [33].

Results and Discussion

Characterizing nZVI

Fig. 1a) shows typical SEM images of the synthesized particles. The particles were composed of spherical particles. A representative single particle size was about 80-150 nm as shown in Fig. 1a). The images also showed that most particles formed chain-like aggregates, which was a common behaviour because of the high surface energies and intrinsic magnetic properties of nanoparticles themselves [34].

The structures of the particles also were characterized by XRD. Fig. 1(b) is the XRD pattern of the particles; it was obvious that the characteristic peaks were at 2θ = 44.9º. The marked XRD characteristic peak at about 44.9º (2θ) belongs to zero valent iron, which had been evidenced by some investigations, so the diffraction peak observed in the composite samples confirms that the formation of iron was zero-valence. Hence, from the results of SEM and XRD, we can conclude that the iron particles were nZVI. There were some broad peaks, suggesting that the surface of iron nanoparticles consists mainly of a layer of iron oxides that possess a chemically disordered crystal structure [35].

The particles were also evaluated by XPS. Fig. 1c) implied that iron seemed to be of three states: one was zero valent state at 706.8 eV, which was for zero valent iron (ZVI), and the other two were oxidation states at 710 and 725 eV. The one at 725 eV was for iron in Fe_3O_4, and the other at 710 eV was at lower oxidation state for Fe(II) [36]. Therefore, the XPS results were in good agreement with those obtained from other technical characterizations of SEM and XRD analysis.

The content of iron in the surface determined by EDS was exhibited in Fig. 1d). EDS analysis confirmed that the iron content is high (up to 83% in the surface of nZVI), further suggesting that iron is the main elemental.

The Oxidative Degradation of NB in nZVI Fenton-like System

Generally, the degradation of organic contaminants with nZVI has been considered to have mainly taken place due to reductive transformation or surface adsorption [37]. Therefore, the degradations of NB in various degradation systems, namely H_2O_2, nZVI, and nZVI Fenton-like systems, were compared to verify the catalytic activity of nZVI and the main process in an nZVI Fenton-like system. Batch experiments were conducted in anoxic glass vessels with 40 mgL^{-1} NB and 150 mgL^{-1} nZVI at initial pH 4.0 to investigate the reduction effect of NB by nZVI. As seen in Fig. 2, about 3.8% of NB was degraded in 240 min at the experiment with 340 mgL^{-1} H_2O_2, because of the antioxidative character of NB and the low
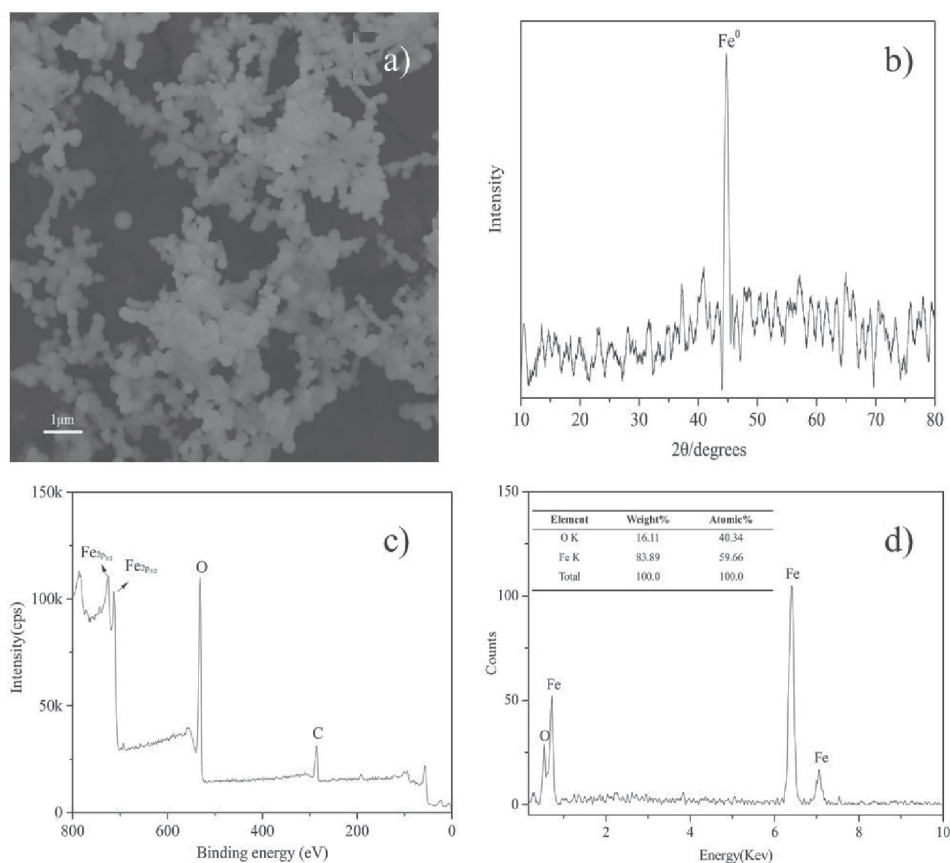
Fig. 1. Characterization of nZVI: a) SEM image, b) XRD pattern, c) XPS spectra, and d) EDS spectrum.

oxidation potential (+1.78 eV) of H_2O_2. The decrease in concentration of NB in nZVI system was about 13.7% in 240 min, indicating that reduction or surface adsorption of nZVI was not effective for NB removal. Nevertheless, when it comes to the experiment with the simultaneous presence of

Fig. 2. Removal curves of NB in H_2O_2, nZVI, and nZVI Fenton-like systems; inset graph is the plots of $\ln(C/C_0)$ versus time for the removal of NB in an nZVI Fenton-like system.

150 mgL^{-1} nZVI and 340 mgL^{-1} H_2O_2, NB in solution was removed fast and 91.9% of NB was removal in 240 min for the generation of hydroxyl radical (HO·) with the oxidation potential of +2.8 eV. The NB removal curves in an nZVI Fenton-like system could be properly fitted by the pseudo first-order kinetics equations ($R_2 = 0.99$, $K = 0.012$ min^{-1}). This result suggested that the nZVI Fenton-like system was effective at NB degradation. Furthermore, the oxidation in an nZVI Fenton-like system played the main role in NB degradation.

The Synergetic Degradation Effect between Homogeneous and Heterogeneous Fenton Processes

It is known that nZVI can serve as a slow-releasing source of dissolved iron ions in an acidic solution [38]. The concentration of dissolved iron ions was monitored during the NB removal in an nZVI Fenton-like system. Then the maximum concentration of dissolved iron was selected for catalysis in the classic Fenton process, and evaluated its potentially largest contribution [39]. As shown in Fig. 3a), the concentration of dissolved iron in nZVI Fenton-like system was gradually increased, and finally reached a maximum value
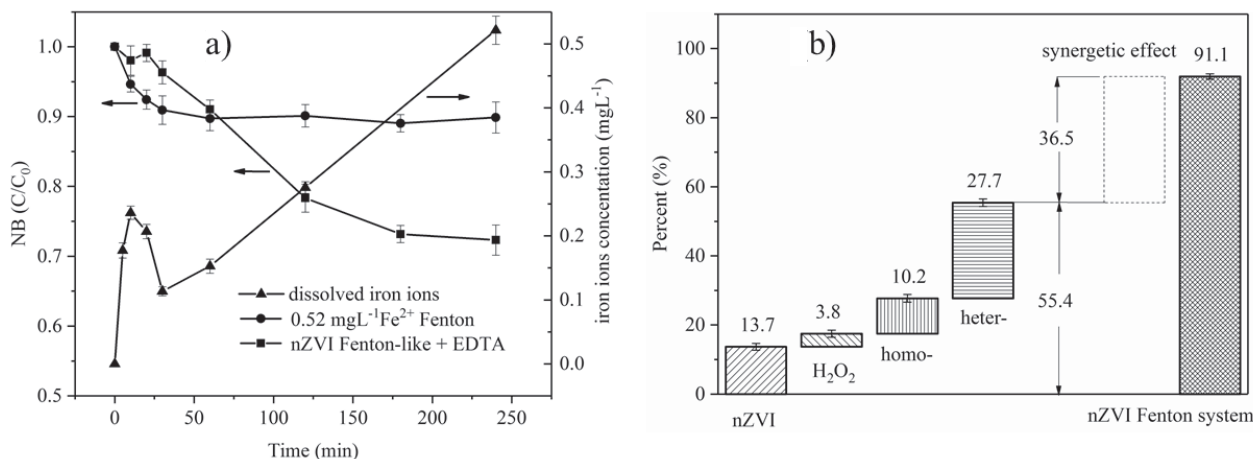
Fig. 3. Investigation of the synergetic degradation effect: a) contributions of heterogeneous and homogeneous Fenton processes to the degradation of NB and b) the synergetic effect on the degradation of NB.

of 0.52 mgL^{-1} at 240 min. As the reaction of NB degradation could be balanced, 0.52 mgL^{-1} was selected as the concentration of a homogeneous catalyst. The effect of a homogeneous Fenton process on the degradation of NB was then investigated in the presence of 0.52 mgL^{-1} Fe^{2+} and 340 mgL^{-1} H_2O_2. Fig. 3 showed that the NB removal efficiency in 60 min could reach 10%, showing an early termination, same as previous studies [40].

As the dissolution of nZVI could not be avoided [38], EDTA was employed as a strong ligand to complex dissolved iron ions to prevent their reactions with hydrogen peroxide or nZVI, and clarify the contribution of a heterogeneous Fenton process in the nZVI Fenton-like system [41]. As shown in Fig. 3a), the degradation of NB was largely depressed by adding EDTA. The removal efficiency of NB only reached about 27.7% within 240 min.

This comparison clearly revealed that the homogeneous Fenton process or heterogeneous Fenton process alone could not induce a great degradation of NB. The higher NB removal efficiency (91.9%) in the nZVI Fenton-like system suggested that the combined effect appeared to be favorable (Fig. 3b). According to previous research results [42, 43], a synergetic degradation effect could exist between homogeneous and heterogeneous Fenton processes.

The Synergetic Catalytic Effect between nZVI and Dissolved Iron Ions

To clarify the origin of the synergetic degradation effect between homogeneous and heterogeneous Fenton processes on NB degradation in an nZVI Fenton-like system, the concentrations of Fe^{2+} were monitored in 0.52 mgL^{-1} Fe^{2+} Fenton, nZVI, and nZVI Fenton-like systems (Fig. 4a). In a 0.52 mgL^{-1} Fe^{2+} Fenton system, most Fe^{2+} were transformed into

Fe^{3+} in 30 min with the presence of H_2O_2 (Eq.(2)) [28]. Although Fe^{3+} could be reduced to form Fe^{2+}, it is too slow in this situation [28]. In the nZVI Fenton-like system, the Fe^{2+} concentration increased rapidly during the first 20 min (Eq. (1)), which has reported that the presence of oxidants could accelerate the corrosion rate of nZVI [44, 45], and then decreased gradually over 60 min. The same phenomenon was found in the nZVI system. After 60 min, the Fe^{2+} concentration in these systems maintained relatively balanced. The Fe^{2+} concentration in an nZVI Fenton-like system remained lower than that in the nZVI system for the presence of H_2O_2, but slightly higher than that in the Fe^{2+} Fenton system, suggesting that the accelerated reduction of Fe^{3+} to Fe^{2+} by nZVI (Eq. 2). In this concentration range, the higher concentration of Fe^{2+}, the faster the decomposition of H_2O_2. The promoted Fe^{3+} and Fe^{2+} redox by nZVI improved the efficiency of homogeneous Fenton process, similar to previous research [28].

To verify the effect of dissolved iron ions on the heterogeneous Fenton process, methanol was employed as the scavenger of HO·, for it has low affinity to oxide surfaces, which means that it can only be oxidized by HO· in the bulk solution [29]. In addition, methanol does not affect the reactions of dissolved iron ions, unlike EDTA. As shown in Fig. 4b), the removal efficiency of NB with the presence of methanol reached about 40% within 240 min. higher about 12% than that with the presence of EDTA. This comparison clearly revealed that the dissolved iron ions could improve the efficiency of the heterogeneous Fenton process. This may be caused by dissolved iron ions speeding up the electrons transfer from an nZVI core to shell, providing surface-bound ferrous ions ($Fe(II)_{bound}$) [29]. These more $Fe(II)_{bound}$ would react with H_2O_2 to produce more HO·, which could be explained by these reactions (Eqs. (4) and (5)):
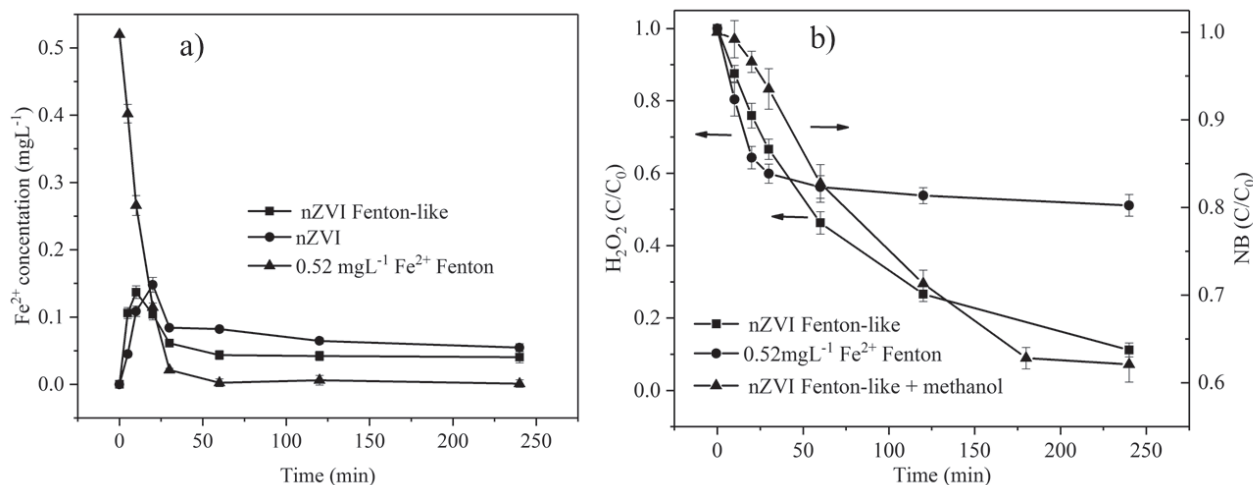
Fig. 4. a) ferrous ion concentrations in nZVI, 0.52 mgL^{-1} Fe^{2+} Fenton, and nZVI Fenton-like systems; and b) concentration of H$_2$O$_2$ in 0.52 mgL^{-1} Fe^{2+} Fenton and nZVI Fenton-like systems, and the removal curves of NB in nZVI Fenton-like system with methanol.

$$Fe(III)_{bound} + e^- \rightarrow Fe(II)_{bound} \quad (4)$$

$$Fe(II)_{bound} + H_2O_2 \rightarrow Fe(III)_{bound} + HO\cdot + OH^- \quad (5)$$
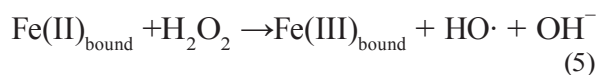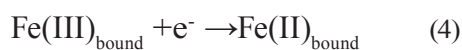
…which clearly revealed that a synergetic catalytic effect between nZVI and dissolved iron ions could exist, which enhanced their catalytic performances and resulted in the synergetic degradation effect between homogeneous and heterogeneous Fenton processes in an nZVI Fenton-like system.

It was noticed that with the same concentration of H$_2$O$_2$, the NB removal efficiencies were different in 0.52 mgL^{-1} Fe^{2+} Fenton and nZVI Fenton-like systems. We therefore monitored the H$_2$O$_2$ concentration changes during the NB degradation in both systems. It could be seen from Fig. 4(b) that the concentration of H$_2$O$_2$ in the 0.52 mgL^{-1} Fe^{2+} Fenton system decreased very quickly with an early termination. The utilization-rate of H$_2$O$_2$ was about 49%. When it came to the nZVI Fenton-like system, the H$_2$O$_2$ was decomposed gradually until it was consumed completely. The concentration of H$_2$O$_2$ decreased slower than that in the 0.52 mgL^{-1} Fe^{2+} Fenton system, but matched better with the NB degradation curve. This H$_2$O$_2$ decomposition comparison revealed that the utilization rate of H$_2$O$_2$ in the nZVI Fenton-
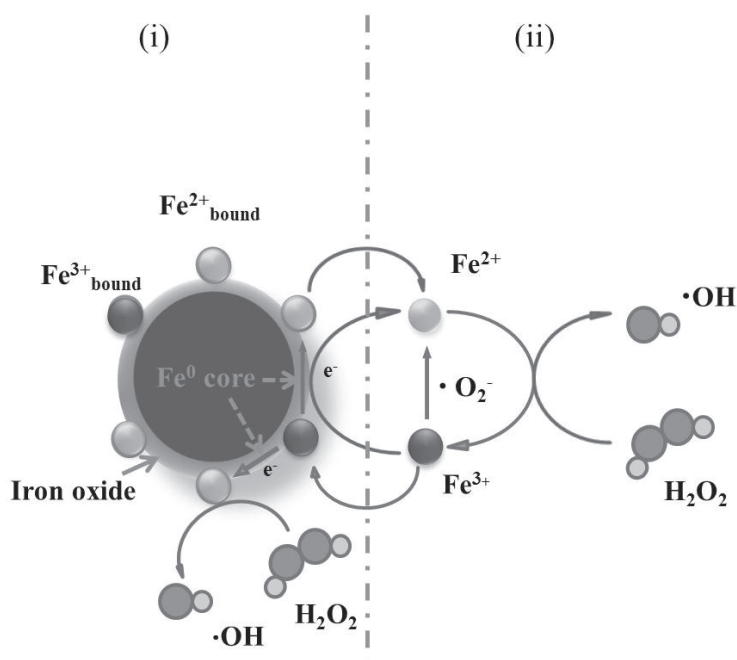
Fig. 5. The possible mechanism of the synergetic effects in the nZVI Fenton-like system.

like system was higher than that in the 0.52 mgL^{-1} Fe^{2+} Fenton system. This could be explained by the presence of nZVI, which proved that electrons reduce Fe^{3+}, which in some way decreased the cost of H$_2$O$_2$ caused by the reduction of Fe(III).

Possible Mechanism of the Synergetic Effects in an nZVI Fenton-like System

On the basis of the above results and analysis, a possible mechanism of the synergetic effects was proposed during NB degradation in the nZVI Fenton-like system shown in Fig. 5i). First, nZVI react with H$^+$ and H$_2$O$_2$ to produce Fe(II)$_{bound}$ and Fe^{2+}, and then H$_2$O$_2$ reacted with Fe(II)$_{bound}$ to produce HO·[29]. Meanwhile, the generated Fe(III)$_{bound}$ were reduced by nZVI. As more and more Fe(II)$_{bound}$ produced, a small fraction of them diffused into the bulk solution as dissolved Fe^{2+} [38], which would cause a homogeneous Fenton reaction (shown as Fig. 5ii)). When the dissolved Fe^{2+} was oxidized by H$_2$O$_2$, the formed Fe^{3+} could also get an electron from the nZVI. The nZVI accelerated the reduction of Fe^{3+} to Fe^{2+}. Thus, the efficiency of the homogeneous Fenton process was improved. On the other hand, the dissolved ferrous ions could not only catalyse the fast decomposition of H$_2$O$_2$, but also enhance the formation of Fe(III)$_{bound}$ by speeding up the electron transfer from nZVI cores to shells, which means the efficiency of the heterogeneous Fenton process was enhanced. The synergetic catalysis effect between nZVI and dissolved iron ions accelerate the efficiency of HO·, which induced the rapidly degradate of NB, showing as a synergetic degradation effect between homogeneous and heterogeneous Fenton processes.

Conclusions

In this study, the synergetic effects in a Fenton-like system were studied using synthesized nano zero-valent iron (nZVI) as catalyst and nitrobenzene (NB) as a model contaminant. The results showed that homogeneous and heterogeneous Fenton processes existed simultaneously in this nZVI Fenton-like system, and a synergetic degradation effect between these processes existed. Through quantitative analysis, 91.2% NB was degraded in 240 min, and 36.5% of NB degradation was attributed to the synergetic degradation effect. This synergetic degradation effect was caused by a synergetic catalytic effect between nZVI and dissolved iron ions (Fe^{3+} and Fe^{2+}). In the bulk solution, the Fe^{3+}/Fe^{2+} redox rate was accelerated by nZVI, resulting in the efficiency improvement of homogeneous catalysis; in the surface of nZVI, these dissolved iron ions promoted the electrons transfer from nZVI core to shell, and enhanced the efficiency of

heterogeneous catalysis. The utilization rate of H$_2$O$_2$ was also improved, because the synergetic catalytic effect reduced the cost of H$_2$O$_2$ caused by reduction of Fe(III). Based on these results, a possible mechanism of synergetic effects in the nZVI Fenton-like system was proposed. These results could provide a promoting insight on the nZVI Fenton-like system, and of course some details still need to be thoroughly researched in further studies.

Conflict of Interest

The authors declare no conflict of interest.

References

1. DIAO Y., YAN Z., GUO M., WANG X. Magnetic multi-metal co-doped magnesium ferrite nanoparticles: An efficient visible light-assisted heterogeneous Fenton-like catalyst synthesized from saprolite laterite ore, J Hazard Mater, **344**, 829, **2018**.
2. TIAN X., JIN H., NIE Y., ZHOU Z., YANG C., LI Y., WANG Y. Heterogeneous Fenton-like degradation of ofloxacin over a wide pH range of 3.6-10.0 over modified mesoporous iron oxide, Chemical Engineering Journal, **328**, 397, **2017**.
3. RODRIGUES C.S.D., SOARES O.S.G.P., PINHO M.T., PEREIRA M.F.R., MADEIRA L.M. p-Nitrophenol degradation by heterogeneous Fenton's oxidation over activated carbon-based catalysts, Applied Catalysis B: Environmental, **219**, 109, **2017**.
4. XU L., WANG J. Magnetic nanoscaled Fe$_3$O$_4$/CeO$_2$ composite as an efficient Fenton-like heterogeneous catalyst for degradation of 4-chlorophenol, Environ Sci Technol, **46** (18), 10145, **2012**.
5. LI W., WANG Y., IRINI A. Effect of pH and H$_2$O$_2$ dosage on catechol oxidation in nano-Fe$_3$O$_4$ catalyzing UV-Fenton and identification of reactive oxygen species, Chemical Engineering Journal, **244**, 1, **2014**.
6. GUO S., ZHANG G., WANG J. Photo-Fenton degradation of rhodamine B using Fe$_2$O$_3$-Kaolin as heterogeneous catalyst: characterization, process optimization and mechanism, J Colloid Interface Sci, **433**, 1, **2014**.
7. JARAMILLO-P EZ C., NAV O J.A., HIDALGO M.C., BOUZIANI A., AZZOUZI M.E. Mixed α-Fe$_2$O$_3$/Bi$_2$WO$_6$ oxides for photoassisted hetero-Fenton degradation of Methyl Orange and Phenol, Journal of Photochemistry and Photobiology A: Chemistry, **332**, 521, **2017**.

8. ZHANG Y., ZHANG K., DAI C., ZHOU X., SI H. An enhanced Fenton reaction catalyzed by natural heterogeneous pyrite for nitrobenzene degradation in an aqueous solution, Chemical Engineering Journal, **244**, 438, **2014**.

9. DIAO Z.H., XU X.R., JIANG D., LI G., LIU J.J., KONG L.J., ZUO L.Z. Enhanced catalytic degradation of ciprofloxacin with FeS_2/SiO_2 microspheres as heterogeneous Fenton catalyst: Kinetics, reaction pathways and mechanism, J Hazard Mater, **327**, 108, **2017**.

10. LIU T., YOU H. Photoassisted Fenton-like degradation of polyacrylamide aqueous solutions using iron oxide/ TiO_2/Al_2O_3 heterogeneous catalysts, Reaction Kinetics, Mechanisms and Catalysis, **109** (1), 233, **2013**.

11. WANG Y., FANG J., CRITTENDEN J.C., SHEN C. Novel RGO/alpha-FeOOH supported catalyst for Fenton oxidation of phenol at a wide pH range using solar-light-driven irradiation, J Hazard Mater, **329**, 321, **2017**.

12. LIU Y., LIU X., ZHAO Y., DIONYSIOU D.D. Aligned α-FeOOH nanorods anchored on a graphene oxide-carbon nanotubes aerogel can serve as an effective Fenton-like oxidation catalyst, Applied Catalysis B: Environmental, **213**, 74, **2017**.

13. SONG R., BAI B., PUMA G.L., WANG H., SUO Y. Biosorption of azo dyes by raspberry-like $Fe_3O4@yeast$ magnetic microspheres and their efficient regeneration using heterogeneous Fenton-like catalytic processes over an up-flow packed reactor, Reaction Kinetics, Mechanisms and Catalysis, **115** (2), 547, **2015**.

14. GOGOI A., NAVGIRE M., SARMA K.C., GOGOI P. Fe_3O_4-CeO_2 metal oxide nanocomposite as a Fenton-like heterogeneous catalyst for degradation of catechol, Chemical Engineering Journal, **311**, 153, **2017**.

15. MIKHAILOV I., KOMAROV S., LEVINA V., GUSEV A., ISSI J.P., KUZNETSOV D. Nanosized zero-valent iron as Fenton-like reagent for ultrasonic-assisted leaching of zinc from blast furnace sludge, J Hazard Mater, **321**, 557, **2017**.

16. YIRSAW B.D., MEGHARAJ M., CHEN Z., NAIDU R. Environmental application and ecological significance of nano-zero valent iron, J Environ Sci (China), **44**, 88, **2016**.

17. BAGAL M.V., GOGATE P.R. Wastewater treatment using hybrid treatment schemes based on cavitation and Fenton chemistry: a review, Ultrason Sonochem, **21** (1), 1, **2014**.

18. YAMAGUCHI R., KUROSU S., SUZUKI M., KAWASE Y. Hydroxyl radical generation by zero-valent iron/Cu (ZVI/Cu) bimetallic catalyst in wastewater treatment: Heterogeneous Fenton/Fenton-like reactions by Fenton reagents formed in-situ under oxic conditions, Chemical Engineering Journal, **334**, 1537, **2018**.

19. VILARDI G., SEBASTIANI D., MILIZIANO S., VERDONE N., DI PALMA L. Heterogeneous nZVI-induced Fenton oxidation process to enhance biodegradability of excavation by-products, Chemical Engineering Journal, **335**, 309, **2018**.

20. FU F., DIONYSIOU D.D., LIU H. The use of zero-valent iron for groundwater remediation and wastewater treatment: a review, J Hazard Mater, **267**, 194, **2014**.

21. LI J., LIU Q., JI Q.Q., LAI B. Degradation of p-nitrophenol (PNP) in aqueous solution by Fe0-PM-PS system through response surface methodology (RSM), Applied Catalysis B: Environmental, **200**, 633, **2017**.

22. JI F., YIN H., ZHANG H., ZHANG Y., LAI B. Treatment of military primary explosives wastewater containing lead styphnate (LS) and lead azide (LA) by mFe0-PS-O3 process, Journal of Cleaner Production, **188**, 860, **2018**.

23. GOMATHI DEVI L., GIRISH KUMAR S., MOHAN REDDY K., MUNIKRISHNAPPA C. Photo degradation of methyl orange an azo dye by advanced Fenton process using zero valent metallic iron: influence of various reaction parameters and its degradation mechanism, J Hazard Mater, **164** (2-3), 459, **2009**.

24. WANG W., ZHOU M., MAO Q., YUE J., WANG X. Novel NaY zeolite-supported nanoscale zero-valent iron as an efficient heterogeneous Fenton catalyst, Catalysis Communications, **11** (11), 937, **2010**.

25. GARRIDO-RAM REZ E.G., THENG B.K.G., MORA M.L. Clays and oxide minerals as catalysts and nanocatalysts in Fenton-like reactions – A review, Applied Clay Science, **47** (3-4), 182, **2010**.

26. WANG Q., TIAN S., NING P. Degradation Mechanism of Methylene Blue in a Heterogeneous Fenton-like Reaction Catalyzed by Ferrocene, Industrial & Engineering Chemistry Research, **53** (2), 643, **2014**.

27. HU S., WU Y., YAO H., LU C., ZHANG C. Enhanced Fenton-like removal of nitrobenzene via internal microelectrolysis in nano zerovalent iron/activated carbon composite, Water Sci Technol, **73** (1), 153, **2016**.

28. SHI J., AI Z., ZHANG L. Fe@Fe2O3 core-shell nanowires enhanced Fenton oxidation by accelerating the Fe(III)/Fe(II) cycles, Water Research, **59**, 145, **2014**.

29. LIU W., AI Z., CAO M., ZHANG L. Ferrous ions promoted aerobic simazine degradation with Fe@Fe_2O_3 core–shell nanowires, Applied Catalysis B: Environmental, **150-151**, 1, **2014**.

30. LEE H., LEE H.J., KIM H.E., KWEON J., LEE B.D., LEE C. Oxidant production from corrosion of nano- and microparticulate zero-valent iron in the presence of oxygen: a comparative study, J Hazard Mater, **265**, 201, **2014**.

31. DU B., SU H., WANG S. Palladium supported on carbon nanofiber coated monoliths for three-phase nitrobenzene hydrogenation: Influence of reduction temperature and oxidation pre-treatment, Journal Of Industrial And Engineering Chemistry, **21**, 997, **2015**.

32. WU Y., YAO H., KHAN S., HU S., WANG L. Characteristics and Mechanisms of Kaolinite-Supported Zero-Valent Iron/H_2O_2 System for Nitrobenzene Degradation, CLEAN - Soil, Air, Water, **45** (3), 1600826, **2017**.

33. FANG G.D., ZHOU D.M., DIONYSIOU D.D. Superoxide mediated production of hydroxyl radicals by magnetite nanoparticles: Demonstration in the degradation of 2-chlorobiphenyl, Journal Of Hazardous Materials, **250-251** (4), 377, **2013**.

34. RONAVARI A., BALAZS M., TOLMACSOV P., MOLNAR C., KISS I., KUKOVECZ A., KONYA Z. Impact of the morphology and reactivity of nanoscale zero-valent iron (NZVI) on dechlorinating bacteria, Water Research, **95**, 165, **2016**.

35. SUN Y.P., LI X.Q., CAO J., ZHANG W.X., WANG H.P. Characterization of zero-valent iron nanoparticles, Advances in Colloid & Interface Science, **120** (1-3), 47, **2006**.

36. KIM S.A., KAMALA-KANNAN S., LEE K.J., PARK Y.J., SHEA P.J., LEE W.H., KIM H.M., OH B.T. Removal of Pb(II) from aqueous solution by a zeolite–nanoscale zero-valent iron composite, Chemical Engineering Journal, **217** (1), 54, **2013**.

37. SHIMIZU A., TOKUMURA M., NAKAJIMA K., KAWASE Y. Phenol removal using zero-valent iron powder in the presence of dissolved oxygen: Roles of

decomposition by the Fenton reaction and adsorption/precipitation, Journal Of Hazardous Materials, **s 201-202** (1), 60, **2012**.

38. XIONG Z., LAI B., YUAN Y., CAO J., YANG P., ZHOU Y. Degradation of p -nitrophenol (PNP) in aqueous solution by a micro-size $Fe0/O_3$ process ($mFe0/O_3$): Optimization, kinetic, performance and mechanism, Chemical Engineering Journal, **302**, 137, **2016**.

39. WANG Q., TIAN S., NING P. Ferrocene-Catalyzed Heterogeneous Fenton-like Degradation of Methylene Blue: Influence of Initial Solution pH, Industrial & Engineering Chemistry Research, **53** (15), 6334, **2014**.

40. MIRZAEI A., CHEN Z., HAGHIGHAT F., YERUSHALMI L. Removal of pharmaceuticals from water by homo/heterogonous Fenton-type processes - A review, Chemosphere, **174**, 665, **2017**.

41. DONG H., HE Q., ZENG G., TANG L., ZHANG L., XIE Y., ZENG Y., ZHAO F. Degradation of trichloroethene by nanoscale zero-valent iron (nZVI) and nZVI activated persulfate in the absence and presence of EDTA, Chemical Engineering Journal, **316**, 410, **2017**.

42. SHI J. On the synergetic catalytic effect in heterogeneous nanocomposite catalysts, Chemical Reviews, **113** (3), 2139, **2013**.

43. XIONG Z., YUAN Y., LAI B., YANG P., ZHOU Y. Mineralization of ammunition wastewater by a micron-size Fe0/O3process ($mFe0/O_3$), RSC Adv., **6** (61), 55726, **2016**.

44. YUAN Y., LAI B., TANG Y.-Y. Combined Fe0/air and Fenton process for the treatment of dinitrodiazophenol (DDNP) industry wastewater, Chemical Engineering Journal, **283**, 1514, **2016**.

45. LI J., JI Q., LAI B., YUAN D. Degradation of p-nitrophenol by $Fe0/H_2O_2$ /persulfate system: Optimization, performance and mechanisms, Journal of the Taiwan Institute of Chemical Engineers, **80**, 686, **2017**.